

ARTICLE

<https://doi.org/10.1038/s41467-019-10800-1>

OPEN

Modulation of extrasynaptic GABA_A alpha 5 receptors in the ventral hippocampus normalizes physiological and behavioral deficits in a circuit specific manner

J.J. Donegan¹, A.M. Boley¹, J. Yamaguchi², G.M. Toney ² & D.J. Lodge ¹

Hippocampal hyperactivity is correlated with psychosis in schizophrenia patients and likely attributable to deficits in GABAergic signaling. Here we attempt to reverse this deficit by overexpression of the $\alpha 5$ -GABA_A receptor within the ventral hippocampus (vHipp). Indeed, this is sufficient to normalize vHipp activity and downstream alterations in dopamine neuron function in the MAM rodent model. This approach also attenuated behavioral deficits in cognitive flexibility. To understand the specific pathways that mediate these effects, we used chemogenetics to manipulate discrete projections from the vHipp to the nucleus accumbens (NAc) or prefrontal cortex (mPFC). We found that inhibition of the vHipp-NAc, but not the vHipp-mPFC pathway, normalized aberrant dopamine neuron activity. Conversely, inhibition of the vHipp-mPFC improved cognitive function. Taken together, these results demonstrate that restoring GABAergic signaling in the vHipp improves schizophrenia-like deficits and that distinct behavioral alterations are mediated by discrete projections from the vHipp to the NAc and mPFC.

¹Department of Pharmacology and Center for Biomedical Neuroscience, University of Texas Health Science Center, San Antonio, TX 78229, USA.

²Department of Cellular and Integrative Physiology and Center for Biomedical Neuroscience, University of Texas Health Science Center, San Antonio, TX 78229, USA. Correspondence and requests for materials should be addressed to J.J.D. (email: Donegan@uthscsa.edu)

Positive symptoms, such as delusions and hallucinations, are often the most striking features of schizophrenia; however, patients also display characteristic cognitive symptoms, such as working memory deficits and cognitive inflexibility, which can negatively influence social and occupational functioning and diminish quality of life^{1–3}. Although the long-standing dopamine hypothesis of schizophrenia suggests that hyperactivity in the mesolimbic dopamine system contributes to disease symptoms⁴, antipsychotic medications, which act as antagonists at the dopamine D2 receptor, are only somewhat effective in treating positive symptoms and have little to no impact on cognitive symptoms of schizophrenia^{1,5}. Further, schizophrenia patients do not display overt pathology in the mesolimbic dopamine system, leading some to suggest that the pathology of schizophrenia lies in upstream brain regions that regulate dopamine signaling⁶.

The hippocampus is one region where functional and anatomical changes have been consistently observed in schizophrenia patients. One of the more reliable observations in schizophrenia patients is increased hippocampal activity at rest⁷. This increase is correlated with positive symptom severity⁸ as well as cognitive dysfunction⁹, suggesting that exaggerated hippocampal activity may be a key pathogenic factor in schizophrenia. The vHipp hyperactivity observed in schizophrenia patients is thought to result from a deficit in GABAergic inhibition⁹. For example, schizophrenia patients show cell loss restricted to specific GABAergic interneuron subtypes (i.e., parvalbumin and somatostatin) in the hippocampus^{10,11}. Previously, we demonstrated that gestational exposure to the mitotoxin methylazoxymethanol (MAM) produces anatomical, physiological, and behavioral deficits that model schizophrenia [for review see ref. 12], including a loss of hippocampal interneurons¹³ and corresponding hippocampal hyperactivity¹⁴, and behavioral correlates of positive¹⁴, negative¹⁵, and cognitive symptoms¹⁵. We further demonstrated that transplanting interneurons derived from embryonic stem cells, normalizes hippocampal activity and attenuates behavioral correlates of positive and cognitive symptoms in the MAM model¹⁵. One way in which GABAergic interneurons regulate the function of pyramidal cells in the hippocampus is via the ionotropic GABA_A receptor, a heteropentameric chloride ion channel. The $\alpha 5$ subunit of the GABA_A receptor is unique in its relatively limited distribution within the hippocampus¹⁶. This subunit has been shown to regulate the timing of pyramidal cell firing, action potential thresholds, and coordinated oscillatory activity¹⁷. Interestingly, hippocampal specific knock-down of the $\alpha 5$ receptor subunit produces impairments that recapitulate positive symptoms of schizophrenia, including deficits in latent inhibition and pre-pulse inhibition^{18,19}. Conversely, systemic $\alpha 5$ agonists normalize dopamine signaling and improve behavioral correlates of positive symptoms in rodent models of schizophrenia²⁰, suggesting that this subunit of the GABA_A receptor may be a viable therapeutic target. However, it is unclear whether enhancing signaling at the $\alpha 5$ GABA_A subunit would also improve cognitive symptoms, which are poorly treated by currently prescribed antidepressants.

Gene therapy holds the promise of treating diseases by replacing defective genes and has been used to target GABAergic signaling in neurological disorders²¹. In the current experiments, we use viral-mediated gene transfer to restore inhibitory signaling in the vHipp by over-expressing the $\alpha 5$ subunit of the GABA_A receptor in pyramidal cells. We found that $\alpha 5$ overexpression increased tonic GABA currents and normalized aberrant pyramidal cell activity in the vHipp. This approach also normalized aberrant dopamine signaling and cognitive function in a rodent model of schizophrenia, suggesting this may be a promising novel treatment strategy for schizophrenia. Next, we identified the

neural circuit mechanisms underlying these effects. Using chemogenetics, we identified the discrete pathways from vHipp that mediate behavioral and physiological deficits that mirror positive and cognitive symptoms of the disorder. Together, these experiments identify a novel approach for treating schizophrenia and provide insight into the anatomical and neurochemical pathways associated with discrete dimensions of schizophrenia, so that therapeutics can be developed with improved efficacy for treating multiple symptom domains.

Results

Effects of $\alpha 5$ overexpression on vHipp neuronal activity. All data are presented as mean \pm SEM. First, to confirm stable transgene expression in the vHipp, we use immunohistochemistry for GFP. As shown in Figure 1a, we observed GFP-labeled cells throughout the pyramidal cell layer of the vHipp. The maximal spread of infection was calculated for a subset of animals to be 2.8 ± 0.57 mm from the site of injection. Further, this GFP expression colocalized with CAMKII staining (Fig. 1b), confirming the selectivity of the CAMKII promoter for pyramidal cells in this brain region. The $\alpha 5$ subunit is predominately located extrasynaptically, while the $\alpha 1$ subunit is primarily found in synapses^{16,22}. Therefore, we used whole-cell patch-clamp recordings to determine if $\alpha 1$ or $\alpha 5$ overexpression was sufficient to augment tonic or phasic activity. We found that over-expressing the $\alpha 5$ subunit in pyramidal cells of the vHipp increased tonic GABA currents without affecting phasic activity. Specifically, we found that $\alpha 5$ overexpression increased the amplitude of tonic GABA currents (Fig. 1c; one-way ANOVA $F_{(2,18)} = 6.84$, $p < 0.05$; Holm–Sidak GFP vs $\alpha 5$ $t = 2.51$, $p < 0.05$; GFP = -19.47 ± 4.29 pA, $\alpha 5 = -44.16 \pm 10.84$ pA; $n = 6–9$ cells per group) while overexpression of the $\alpha 1$ subunit had no effect on tonic current amplitude (Holm–Sidak GFP vs $\alpha 1$ $t = 1.03$, $p > 0.05$; $\alpha 1 = -9.71 \pm 3.74$ pA). Neither IPSC amplitude nor frequency were affected by either $\alpha 1$ or $\alpha 5$ overexpression in hippocampal slice preparations (Fig. 1c; IPSC amplitude: one-way ANOVA $F_{(2,21)} = 0.30$, $p > 0.05$; Holm–Sidak GFP vs $\alpha 1$ $t = 0.07$, $p > 0.05$; Holm–Sidak GFP vs $\alpha 5$ $t = 0.67$, $p > 0.05$; GFP = -54.07 ± 4.80 pA, $\alpha 1 = -53.40 \pm 4.78$ pA, $\alpha 5 = -60.31 \pm 10.45$ pA; IPSC frequency: one-way ANOVA $F_{(2,21)} = 0.17$, $p > 0.05$; Holm–Sidak GFP vs $\alpha 1$ $t = 0.58$, $p > 0.05$; Holm–Sidak GFP vs $\alpha 5$ $t = 0.16$, $p > 0.05$; GFP = 1.05 ± 0.28 Hz, $\alpha 1 = 0.83 \pm 0.30$ Hz, $\alpha 5 = 0.98 \pm 0.21$ Hz). Representative traces are shown in Fig. 1d and images of recorded cells are shown in (1e) and (1f).

Next, we determined if overexpression of the $\alpha 1$ or $\alpha 5$ subunit of the GABA_A receptor produces functional changes in *in vivo* vHipp pyramidal cell activity using extracellular electrophysiology. Consistent with the *in vitro* data, we demonstrate that $\alpha 5$, but not $\alpha 1$, overexpression normalizes the aberrant vHipp activity observed in the MAM model (Fig. 1g; two-way ANOVA: Interaction $F_{(1,326)} = 4.73$, $p < 0.05$; Prenatal Treatment $F_{(1,326)} = 0.10$, $p > 0.05$; Gene Therapy $F_{(1,326)} = 2.40$, $p > 0.05$; $n = 43–62$ cells per group). Specifically, as we have seen previously¹⁵, MAM-treated rats have an increase in pyramidal cell firing rate in the vHipp compared to saline controls (saline/GFP = 0.68 ± 0.08 Hz, MAM/GFP = 0.89 ± 0.07 Hz; Holm–Sidak saline/GFP vs MAM/GFP $t = 2.06$, $p < 0.05$). In MAM-treated rats that received the virus to over-express the $\alpha 5$ subunit of the GABA_A receptor, this effect was completely abolished (MAM/ $\alpha 5$ = 0.52 ± 0.07 Hz; Holm–Sidak MAM/GFP vs MAM/ $\alpha 5$ $t = 3.84$, $p < 0.05$). In saline-treated rats, $\alpha 5$ overexpression had no effect on pyramidal cell firing rate in the vHipp (saline/ $\alpha 5$ = 0.74 ± 0.07 Hz; Holm–Sidak saline/GFP vs saline/ $\alpha 5$ $t = 0.56$, $p > 0.05$). Over-expression of the $\alpha 1$ subunit had no effect in either the saline- or the MAM-treated animals (saline/ $\alpha 1$ = 0.68 ± 0.07 Hz,

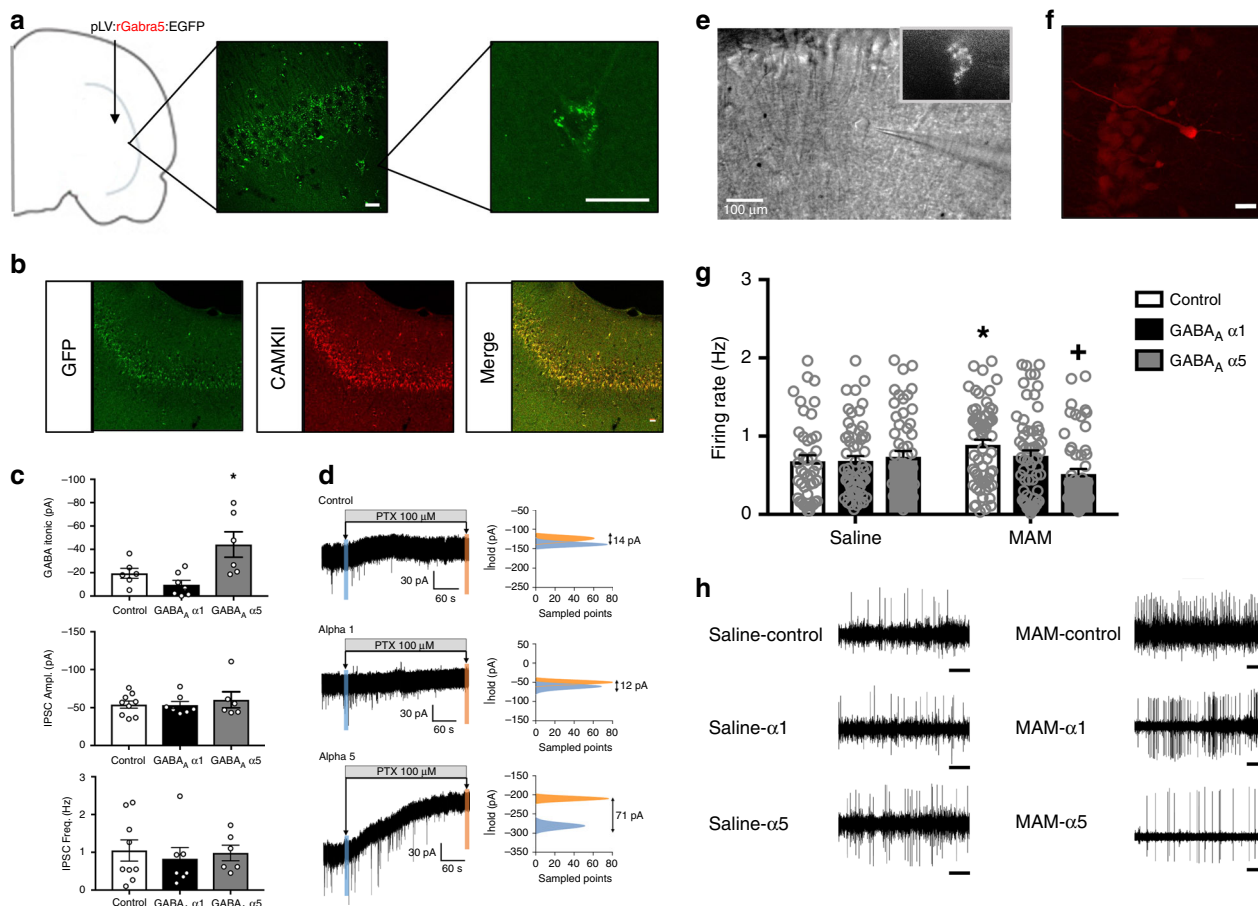


Fig. 1 $\alpha 5$ overexpression reduces tonic currents and firing rates in vHipp pyramidal cells. The placement of virus injections are indicated on a schematic of a coronal section through the vHipp. Circles indicate injections of the control virus. Squares indicate injections of the GABA_A virus. Immunohistochemistry for GFP was used to confirm transgene expression in the vHipp. Representative images are shown in **a**. To verify that gene expression was confined primarily to CAMKII-positive pyramidal cells, we also performed dual-labelling for GFP and CAMKII. Representative images are shown in **b**. Overexpression of the $\alpha 5$, but not the $\alpha 1$, subunit of the GABA_A receptor increased tonic GABA currents (**c**). Neither $\alpha 1$ nor $\alpha 5$ overexpression affected IPSC frequency or amplitude (**c**). Representative traces are shown in **d**. A representative GFP-positive cell is depicted in **e**. A subset of recorded cells were labeled with neurobiotin and a representative image of a neurobiotin-labeled pyramidal cell is shown in **f**. Scale bars are 20 microns unless otherwise labeled. Asterisk is significantly different than control using One-way ANOVA and Holm-Sidak tests. $n = 6-9$ cells per group. Extracellular electrophysiology was used to measure the firing rates of putative pyramidal cells in the vHipp. In the MAM model of schizophrenia, there is an increase in pyramidal cell firing rate, which is completely abolished by overexpression of the $\alpha 5$, but not $\alpha 1$ subunit of the GABA_A receptor (**g**). Representative traces are shown in **h**. Scale bar is 5 s. Asterisk is significantly different than saline/control; +plus is significantly different than MAM/control using Two-Way ANOVA and Holm-Sidak tests. $n = 43-62$ cells per group. Data are shown as mean \pm SEM

MAM/ $\alpha 1 = 0.75 \pm 0.07$ Hz; Holm-Sidak saline/GFP vs saline/ $\alpha 1$ $t = 0.05$, $p > 0.05$; Holm-Sidak MAM/GFP vs MAM/ $\alpha 1$ $t = 1.51$, $p > 0.05$). Representative electrophysiology traces are depicted in Fig. 1h. Together, these results suggest that gene therapy can be used to increase $\alpha 5$ expression in pyramidal cells of the vHipp and this overexpression has functional consequences for pyramidal cell activity.

Effects of $\alpha 5$ overexpression on VTA neuronal activity.

Although it is difficult to model delusions and hallucinations in a rodent, these positive symptoms have been attributed to increases in dopamine neurotransmission⁶. Therefore, we used in vivo extracellular electrophysiology to measure dopamine cell activity as a proxy for positive symptoms and found that overexpression of the $\alpha 5$ subunit of the GABA_A receptor in the vHipp can normalize aberrant dopamine population activity in the VTA (Fig. 2b; two-way ANOVA: Interaction $F_{(1,24)} = 12.43$, $p < 0.05$; Prenatal Treatment $F_{(1,24)} = 19.18$, $p < 0.05$; Gene

Therapy $F_{(1,24)} = 24.25$, $p < 0.05$; $n = 6-7$ rats per group). As we have shown previously¹⁵, MAM-treated animals have an increase in the number of spontaneously active dopamine cells per track compared to saline-treated control animals (saline/GFP = 1.09 ± 0.09 cells/track; MAM/GFP = 1.77 ± 0.09 cells/track; Holm-Sidak saline/GFP vs MAM/GFP $t = 5.49$, $p < 0.05$). This effect is attenuated in MAM-treated animals when the $\alpha 5$ subunit of the GABA_A receptor is over-expressed in pyramidal cells of the vHipp (MAM/ $\alpha 5 = 1.05 \pm 0.09$ cells/track; Holm-Sidak MAM/GFP vs MAM/ $\alpha 5$ $t = 5.87$, $p < 0.05$). Dopamine cell population activity was not affected by $\alpha 5$ overexpression in saline-treated controls (Saline/ $\alpha 5 = 0.98 \pm 0.08$ cells; Holm-Sidak saline/GFP vs saline/ $\alpha 5$ $t = 1.01$, $p > 0.05$). We also analyzed two additional parameters of dopamine cell activity: firing rate and the percentage of action potentials fired in bursts. We found that overexpression of the $\alpha 5$ subunit in the vHipp affected firing rate (Fig. 2c; two-way ANOVA: Interaction $F_{(1,23)} = 2.522$, $p > 0.05$; Prenatal Treatment $F_{(1,23)} = 0.05$, $p > 0.05$; Gene Therapy $F_{(1,23)} = 4.52$, $p < 0.05$). In the

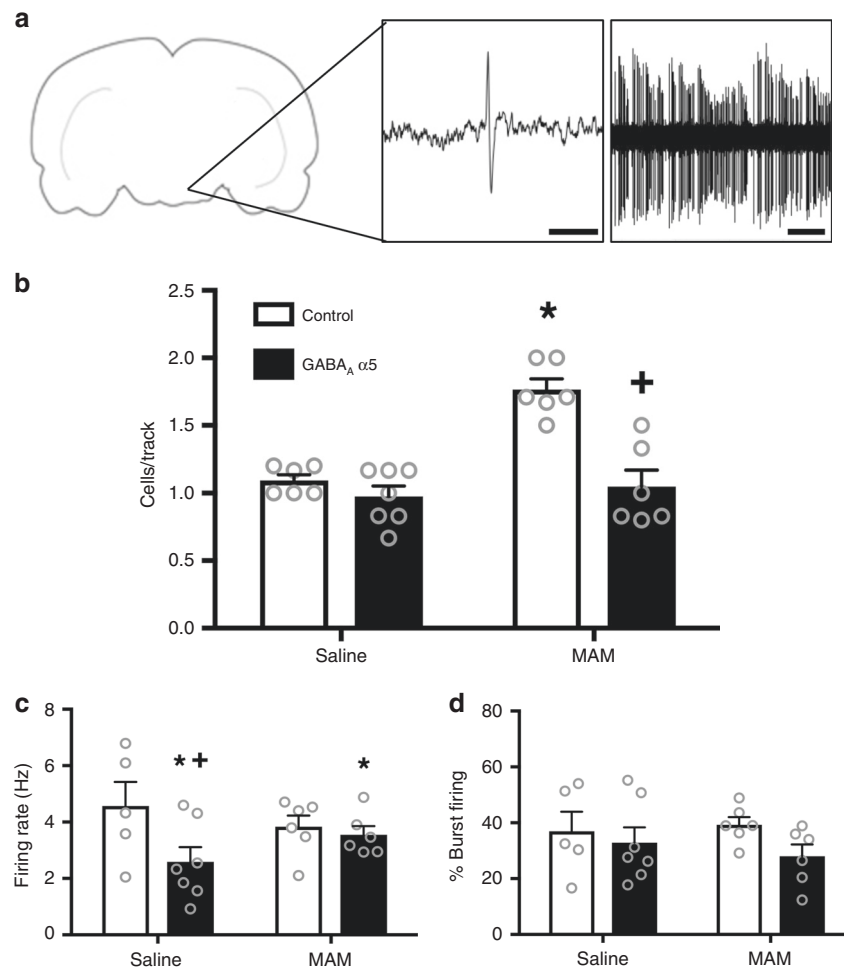


Fig. 2 $\alpha 5$ overexpression normalizes dopamine cell activity in the MAM model of schizophrenia. Extracellular electrophysiology was used to record dopamine cell activity in the VTA. Representative traces are shown in **a**. In the MAM model of schizophrenia, the increase in the number of spontaneously active dopamine cells is attenuated by overexpression of the $\alpha 5$ subunit in pyramidal cells of the vHipp (**b**). Asterisk is significantly different than saline/control; +plus is significantly different than MAM/control. The average firing rate of dopamine cells was decreased by $\alpha 5$ overexpression in both saline- and MAM-treated animals (**c**). Asterisk is significantly different than saline; +plus is significantly different than saline/control. The percentage of cells firing in a burst pattern was not affected by either MAM treatment or by $\alpha 5$ overexpression (**d**). $n = 6-7$ rats per group. Scale bar is 10 ms. All data were analyzed using Two-Way ANOVA and Holm-Sidak tests. Data are shown as mean \pm SEM

saline-treated animals, the $\alpha 5$ overexpression produced a significant decrease in dopamine cell firing rate compared to animals that received the control virus (saline/GFP = 4.57 ± 0.58 Hz; saline/ $\alpha 5$ = 2.59 ± 0.49 Hz; Holm-Sidak saline/GFP vs saline/ $\alpha 5$ $t = 2.608$, $p < 0.05$). In the MAM-treated animals, gene therapy had no effect on the firing rate of dopamine neurons (MAM/GFP = 3.84 ± 0.53 Hz; MAM/ $\alpha 5$ = 3.55 ± 0.53 Hz; Holm-Sidak MAM/GFP vs MAM/ $\alpha 5$ $t = 0.38$, $p > 0.05$). Overexpression of the $\alpha 5$ subunit of the GABA_A receptor in the vHipp had no effect on the bursting activity of dopamine neurons in the VTA (Fig. 2d; two-way ANOVA: Interaction $F_{(1,23)} = 0.52$, $p > 0.05$; Prenatal Treatment $F_{(1,23)} = 0.06$, $p > 0.05$; Gene Therapy $F_{(1,23)} = 2.35$, $p > 0.05$; saline/GFP = $36.97 \pm 5.45\%$ bursting; saline/ $\alpha 5$ = $32.89 \pm 4.61\%$ bursting; MAM/GFP = $39.33 \pm 4.98\%$ bursting; MAM/ $\alpha 5$ = $28.05 \pm 4.98\%$ bursting). Representative traces are shown in Fig. 2a. Together, these results suggest that gene therapy to increase expression of the $\alpha 5$ subunit of the GABA_A receptor in pyramidal cells of the vHipp normalizes activity in the dopamine system and may attenuate the dopamine-related positive symptoms of schizophrenia.

$\alpha 5$ overexpression improves cognitive function. Reversal learning is one form of cognitive flexibility that is disrupted in schizophrenia²³. Using the attentional set-shifting test, we demonstrated that MAM-treated animals also show a deficit in reversal learning, which was not affected by gene therapy (Fig. 3a; two-way ANOVA: Interaction $F_{(1,22)} = 0.04$, $p > 0.05$; Prenatal Treatment $F_{(1,22)} = 26.28$, $p < 0.05$; Gene Therapy $F_{(1,22)} = 0.62$, $p > 0.05$; $n = 5-7$ rats per group). Specifically, we found that MAM-treated animals show an increase in trials to meet criterion compared to saline-treated controls (saline/GFP = 12.5 ± 1.56 trials; MAM/GFP = 20.40 ± 1.71 trials; Holm-Sidak saline/GFP vs MAM/GFP $t = 3.42$, $p < 0.05$). The MAM-induced deficit on reversal learning was not attenuated by overexpression of the $\alpha 5$ subunit of the GABA_A receptor (saline/ $\alpha 5$ = 13.43 ± 1.44 trials; MAM/ $\alpha 5$ = 22.0 ± 1.71 trials; Holm-Sidak saline/ $\alpha 5$ vs MAM/ $\alpha 5$ $t = 3.84$, $p < 0.05$). Further, $\alpha 5$ overexpression had no effect on reversal learning in the saline-treated group (Holm-Sidak saline/GFP vs saline/ $\alpha 5$ $t = 0.44$, $p > 0.05$).

In addition to reversal learning deficits, schizophrenia patients also show deficits in extradimensional set-shifting²³, a higher order form of cognitive flexibility that is critically dependent on

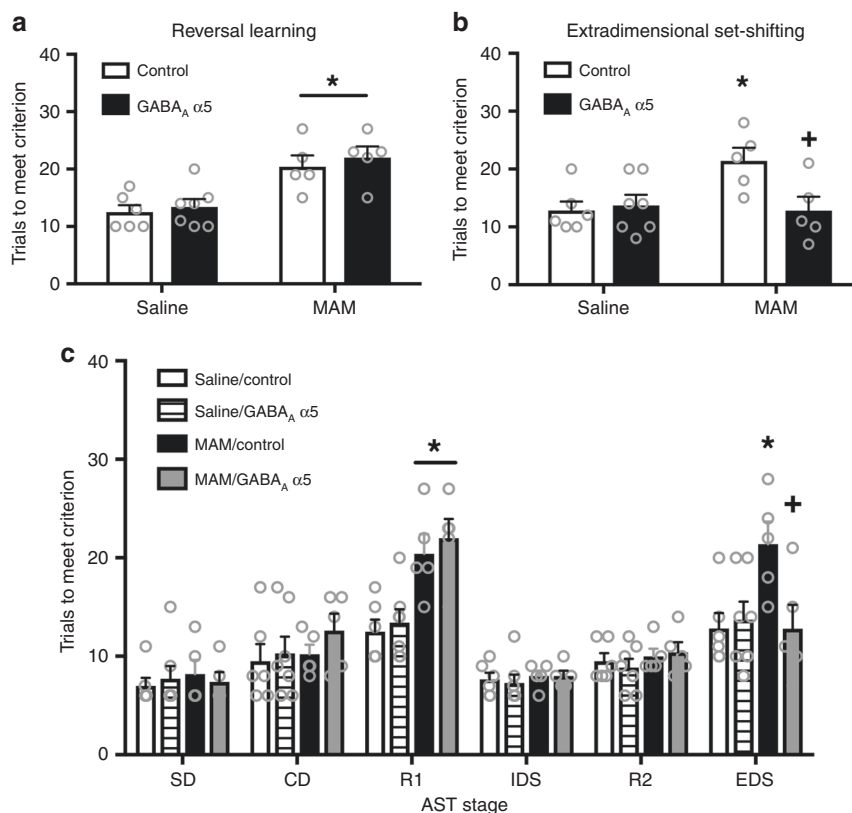


Fig. 3 $\alpha 5$ overexpression improves some forms of cognitive flexibility in the MAM model. The attentional set-shifting test (AST) was used to measure reversal learning and extradimensional set-shifting (ED), two forms of cognitive flexibility. The MAM-induced deficit in reversal learning was not affected by over-expressing the $\alpha 5$ subunit in the vHipp (**a**). Asterisk is a significant main effect compared to saline. The deficit in extradimensional set-shifting caused by MAM treatment is completely abolished by gene therapy to over-express the $\alpha 5$ subunit of the GABA_A receptor (**b**). Asterisk is significantly different than saline/control; +plus is significantly different than MAM/control. All stages of the AST are shown in **c**. SD is simple discrimination. CD is compound discrimination. R1 is the first reversal. IDS is intradimensional set-shift. R2 is the second reversal. EDS is the extradimensional set-shift. $n = 5$ –7 rats per group. All data were analyzed using Two-Way ANOVA and Holm–Sidak tests. Data are shown as mean \pm SEM

the medial prefrontal cortex (mPFC)²⁴. Unlike reversal learning, we found that gene therapy to over-express the $\alpha 5$ subunit of the GABA_A receptor improves schizophrenia-like deficits in extradimensional set-shifting as measured by the attentional set-shifting test (Fig. 3b; two-way ANOVA: Interaction $F_{(1,21)} = 6.02$, $p < 0.05$; Prenatal Treatment $F_{(1,21)} = 2.92$, $p > 0.05$; Gene Therapy $F_{(1,21)} = 2.97$, $p > 0.05$; $n = 5$ –7 rats per group). As we have shown previously¹⁵, MAM-treated animals have a deficit in extradimensional set-shifting as evidenced by an increase in trials to meet criterion compared to controls (saline/GFP = 12.83 ± 1.96 trials; MAM/GFP = 21.40 ± 2.15 trials; Holm–Sidak saline/GFP vs MAM/GFP $t = 2.94$, $p < 0.05$). This deficit was completely abolished in the animals that received gene therapy to over-express the $\alpha 5$ subunit in pyramidal cells of the vHipp (saline/ $\alpha 5$ = 14.33 ± 1.96 trials; MAM/ $\alpha 5$ = 12.8 ± 2.15 trials; Holm–Sidak saline/ $\alpha 5$ vs MAM/ $\alpha 5$ $t = 0.53$, $p > 0.05$). The $\alpha 5$ overexpression had no effect in the saline-treated controls (Holm–Sidak saline/GFP vs saline/ $\alpha 5$ $t = 0.54$, $p > 0.05$). No other stages of the AST were affected by MAM treatment or $\alpha 5$ overexpression (Fig. 3c), suggesting that there was not a deficit in basic learning or memory processes. Together, these results suggest that gene therapy to increase $\alpha 5$ expression in the vHipp may be an effective treatment strategy to alleviate both positive and cognitive deficits associated with schizophrenia.

The vHipp-NAc pathway mediates aberrant dopamine activity.

We have previously demonstrated that the increase in dopamine

population activity is directly attributable to a pathologically enhanced drive from the vHipp¹⁴. However, the vHipp does not project directly to the VTA; therefore, in the current experiments, we demonstrate that reducing activity in the vHipp-NAc pathway of MAM-treated animals abolishes the MAM-induced increase in dopamine population activity (Fig. 4f; two-way ANOVA: Interaction $F_{(1,19)} = 15.98$, $p < 0.05$; Prenatal treatment $F_{(1,19)} = 12.04$, $p < 0.05$; DREADD condition $F_{(1,19)} = 6.607$, $p < 0.05$; $n = 4$ –5 rats per group). In line with our previous findings, MAM-treated animals show a significant increase in the number of spontaneously active dopamine cells per track (saline/GFP = 0.90 ± 0.14 cells per track, MAM/GFP = 1.95 ± 0.14 cells per track; Holm–Sidak saline/GFP vs MAM/GFP $t = 5.28$, $p < 0.05$). Chemogenetic inhibition of the vHipp-NAc pathway attenuated the increase in dopamine population activity in MAM-treated animals but had no effect in controls (saline/Gi = 1.10 ± 0.14 cells per track, MAM/Gi = 1.03 ± 0.14 cells per track; Holm–Sidak MAM/GFP vs MAM/Gi: $t = 4.64$, $p < 0.05$; Holm–Sidak saline/GFP vs saline/Gi: $t = 1.01$, $p > 0.05$). The firing rate (Fig. 4g; two-way ANOVA: Interaction $F_{(1,19)} = 1.161$, $p > 0.05$; Prenatal treatment $F_{(1,19)} = 0.52$, $p > 0.05$; DREADD condition $F_{(1,19)} = 0.59$, $p > 0.05$; saline/GFP = 2.6 ± 0.61 Hz, saline/Gi = 3.73 ± 0.61 Hz; MAM/GFP = 3.70 ± 0.61 Hz, MAM/Gi = 3.51 ± 0.61 Hz) and burst pattern (Fig. 4h; two-way ANOVA: Interaction $F_{(1,19)} = 1.74$, $p > 0.05$; Prenatal treatment $F_{(1,19)} = 0.10$, $p > 0.05$; DREADD condition $F_{(1,19)} = 0.65$, $p > 0.05$; saline/GFP = $65.83 \pm 11.12\%$, saline/Gi = $42.22 \pm 11.12\%$; MAM/GFP = $47.58 \pm$

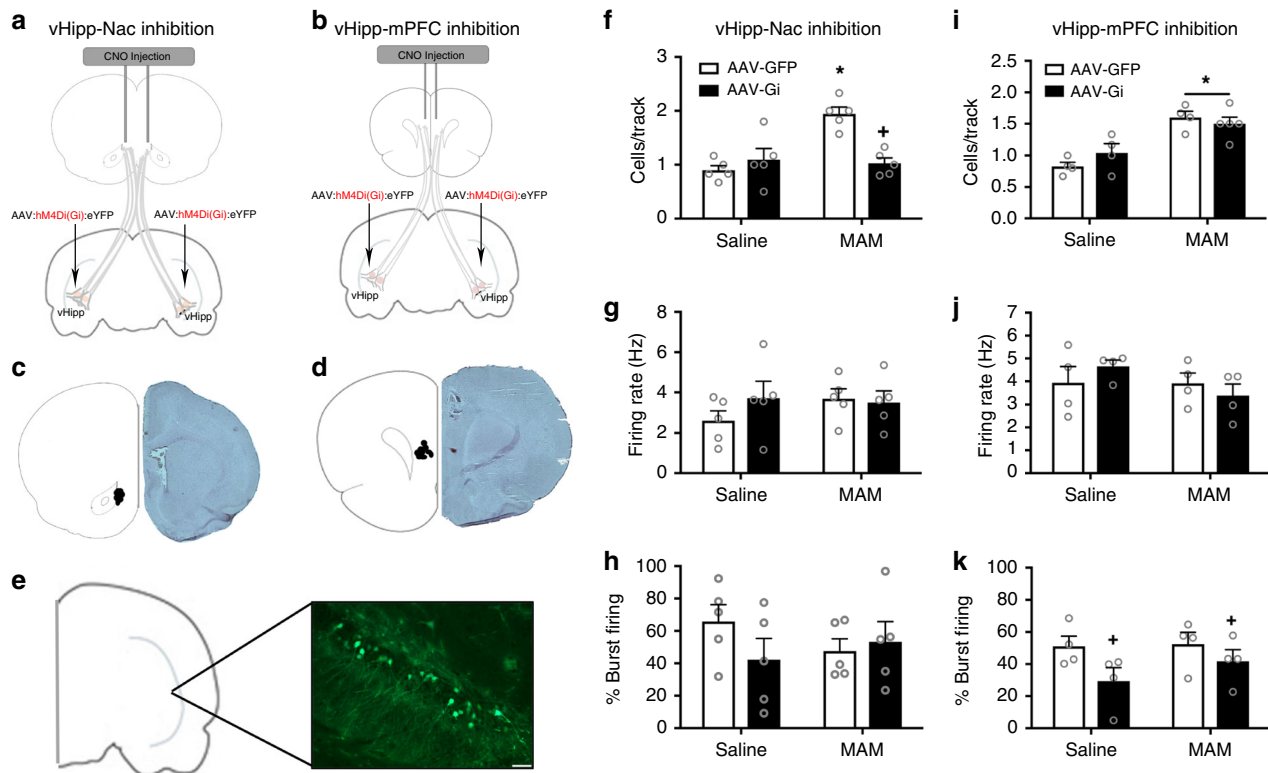


Fig. 4 Inactivation of the vHipp-NAc normalizes dopamine population activity in MAM-treated rats. The schematic depicting the strategy used for pathway inhibition is shown in **a, b**. An adeno-associated virus that expressed the Gi DREADD was injected into the vHipp. At the time of testing, CNO was injected directly into the NAc (**a**) or mPFC (**b**). Cartoon showing the location of the CNO injection and micrograph of representative section are shown in **c, d**. DREADD expression in pyramidal cells of the vHipp was confirmed using immunohistochemistry and a representative image is shown in **e**⁷⁰. $n = 3$ rats per group. Scale bar is 50 microns. MAM-treated animals show an increase in the number of spontaneously active dopamine cells per track in the VTA compared to saline controls. Chemogenetic inactivation of vHipp afferents to the NAc completely abolishes the MAM-induced increase in dopamine population activity (**f**). Neither firing rate (**g**) nor the percentage of action potentials fired in bursts (**h**) were affected by MAM treatment or pathway inhibition. $n = 5$ rats per group. Asterisk is significantly different from saline/GFP; +plus is significantly different than MAM/GFP. The MAM-induced increase in dopamine cell population activity is not affected by inhibition of the vHipp to mPFC pathway (**i**). Neither MAM treatment nor pathway inhibition affect firing rate (**j**). The percentage of action potentials fired in a burst pattern was decreased by vHipp-mPFC pathway inhibition in both the saline- and MAM-treated animals (**k**). $n = 4-5$ rats per group. Asterisk is significantly different from saline; +plus is significantly different than GFP. All data were analyzed using Two-Way ANOVA and Holm-Sidak tests. Data are shown as mean \pm SEM

11.12%, MAM/Gi = $53.29 \pm 11.12\%$) of VTA dopamine cells were not affected by either MAM treatment or pathway inhibition.

Conversely, inhibition of the vHipp-mPFC pathway has no effect on dopamine cell firing in the VTA (Fig. 4i; two-way ANOVA: Interaction $F_{(1,16)} = 2.17$, $p > 0.05$; Prenatal treatment $F_{(1,16)} = 32.76$, $p < 0.05$; DREADD condition $F_{(1,16)} = 0.29$, $p > 0.05$; $n = 4-5$ per group). Although MAM-treated animals showed a significant increase in the number of spontaneously active dopamine cells per track (saline/GFP = 0.83 ± 0.11 cells per track, MAM/GFP = 1.60 ± 0.11 cells per track; Holm-Sidak saline/GFP vs MAM/GFP $t = 4.96$, $p < 0.05$), inhibition of the vHipp-mPFC pathway did not normalize dopamine population activity (saline/Gi = 1.04 ± 0.11 cells per track, MAM/Gi = 1.50 ± 0.10 cells per track; Holm-Sidak MAM/GFP vs MAM/Gi $t = 0.68$, $p > 0.05$). Firing rate was not affected by either prenatal treatment or pathway inhibition (Fig. 4j); two-way ANOVA: Interaction $F_{(1,15)} = 1.508$, $p > 0.05$; Prenatal treatment $F_{(1,15)} = 1.62$, $p > 0.05$; DREADD condition $F = 0.03$, $p > 0.05$; saline/GFP = 3.93 ± 0.51 Hz, MAM/GFP = 3.91 ± 0.51 Hz, Saline/Gi = 4.66 ± 0.51 Hz, MAM/Gi = 3.37 ± 0.51 Hz). There was a main effect of the Gi DREADD on the percentage of action potentials fired in bursts (Fig. 4k; two-way ANOVA: Interaction $F_{(1,15)} = 0.55$, $p > 0.05$; Prenatal treatment $F_{(1,15)} = 0.87$, $p > 0.05$; DREADD condition

$F = 4.79$, $p < 0.05$; saline/GFP = $51.01 \pm 7.38\%$, MAM/GFP = $52.41 \pm 7.38\%$, Saline/Gi = $29.37 \pm 7.38\%$, MAM/Gi = $41.74 \pm 7.38\%$). Cannula placements are shown in Fig. 4c, d and a representative image of DREADD expression is shown in Fig. 4e.

Together, these results suggest that hyperactivity in the vHipp-NAc pathway, but not the vHipp-mPFC pathway, underlies the increase in dopamine cell population activity observed in the MAM model of schizophrenia.

The vHipp-NAc pathway mediates deficits in reversal learning.

To identify the neural pathways involved in unique forms of cognitive flexibility, we used the attentional set-shifting test. We found that hyperactivity in the vHipp-NAc pathway is responsible for reversal learning deficits in the MAM model of schizophrenia (Fig. 5a; two-way ANOVA: Interaction $F_{(1,26)} = 1.68$, $p > 0.05$; Prenatal treatment $F_{(1,26)} = 10.11$, $p < 0.05$; DREADD Condition $F_{(1,26)} = 8.38$, $p < 0.05$; $n = 6-7$ per group). Specifically, we found that MAM treatment produced a deficit in reversal learning, as evidenced by an increase in trials to meet criterion (saline/GFP = 14.67 ± 1.77 trials to meet criterion, MAM/GFP = 22.14 ± 1.64 trials; Holm-Sidak saline/GFP vs MAM/GFP $t = 3.10$, $p < 0.05$). The reversal learning deficit was

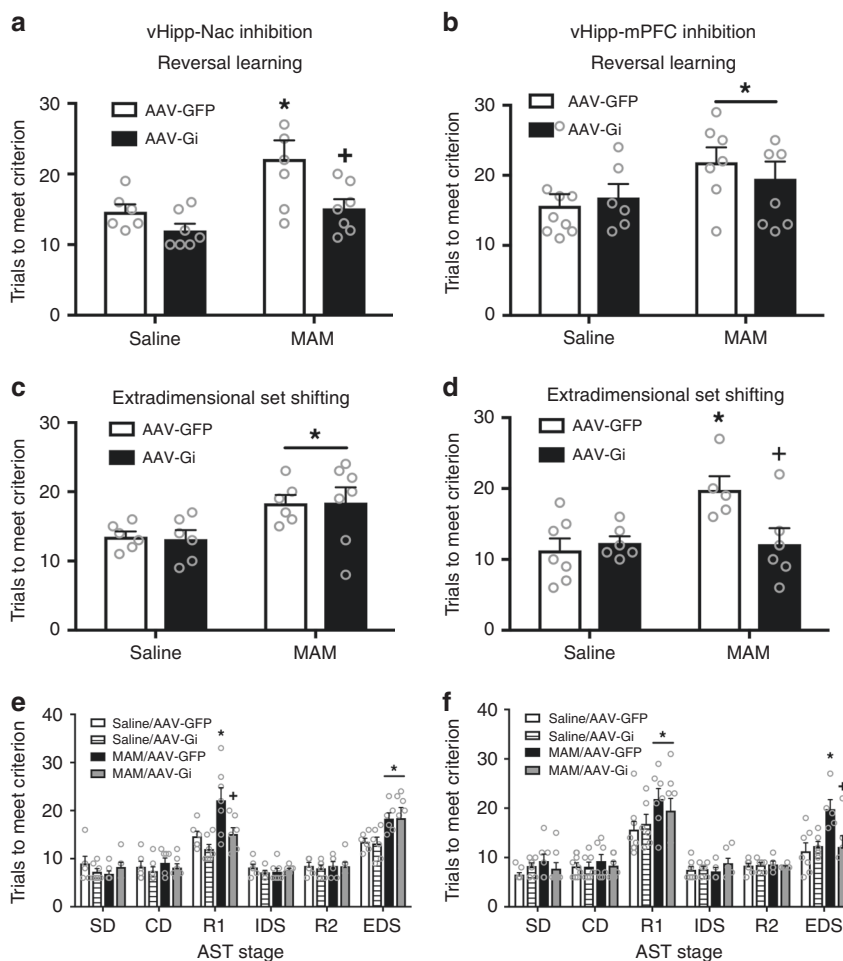


Fig. 5 vHipp-Nac and vHipp-mPFC pathways differentially affect distinct types of cognitive flexibility. MAM treatment causes a deficit in both reversal learning and in extradimensional set-shifting. Inhibition of the vHipp-Nac pathway completely abolishes the MAM-induced deficit in reversal learning (a). Asterisk is significantly different than saline/GFP. Plus is significantly different than MAM/GFP. However, vHipp-Nac inhibition had no effect on extradimensional set-shifting (c). Asterisk is significant main effect of MAM. *n* = 6–7 rats per group. Conversely, inhibition of the vHipp-mPFC pathway had no effect on reversal learning performance (b). Asterisk is significant main effect of MAM. *n* = 6–9 rats per group. However, vHipp-mPFC inhibition did attenuate the MAM-induced deficit in extradimensional set-shifting (d). Asterisk is significantly different than saline/GFP; plus is significantly different than MAM/GFP. *n* = 6–7 rats per group. All stages of the AST are shown in e, (f). All data were analyzed using Two-Way ANOVA and Holm–Sidak tests. Data are shown as mean ± SEM

attenuated by inhibition of the vHipp-Nac pathway (MAM/Gi = 15.14 ± 1.64; Holm–Sidak MAM/GFP vs MAM/Gi *t* = 3.03, *p* < 0.05; Holm–Sidak Saline/Gi vs MAM/Gi *t* = 1.36, *p* > 0.05). Inhibition of the vHipp-Nac pathway had no effect on reversal learning performance in the saline-treated rats (saline/Gi = 12.00 ± 1.64; Holm–Sidak saline/GFP vs saline/Gi *t* = 1.11, *p* > 0.05).

Conversely, we found that reversal learning was not affected by inhibition of the vHipp-mPFC pathway (Fig. 5b; two-way ANOVA: Interaction $F_{(1,29)} = 0.71$, *p* > 0.05; Prenatal treatment $F_{(1,29)} = 4.46$, *p* < 0.05; DREADD condition $F_{(1,29)} = 0.0806$, *p* > 0.05; *n* = 6–7 per group). MAM-treated rats required significantly higher trials to reach criterion than saline-treated controls (saline/GFP = 15.67 ± 1.89 trials, MAM/GFP = 21.86 ± 2.145 trials; Holm–Sidak saline/GFP vs MAM/GFP *t* = 0.04, *p* < 0.05). The MAM-induced deficit was not altered by inhibition of the vHipp-mPFC pathway (saline/Gi = 16.83 ± 2.32 trials, MAM/Gi = 19.50 ± 2.01 trials; Holm–Sidak saline/Gi vs MAM/Gi *t* = 0.87, *p* > 0.05). Together, these results suggest that hyperactivity in the vHipp-Nac pathway, but not the vHipp-mPFC pathway contributes to the reversal learning deficits observed in the MAM model of schizophrenia.

The vHipp-mPFC pathway mediates set-shifting deficits.

Unlike reversal learning, we found that extradimensional set-shifting deficits are not affected by inhibition of the vHipp-Nac pathway (Fig. 5c; two-way ANOVA: Interaction $F_{(1,24)} = 0.02$, *p* > 0.05; Prenatal treatment $F_{(1,24)} = 10.49$, *p* < 0.05; DREADD Condition $F_{(1,24)} = 0.01$, *p* > 0.05; *n* = 6–7 per group). As seen previously, we found that MAM-treated animals have a deficit in extradimensional set-shifting as evidenced by an increase in trials to meet criterion (saline/GFP = 13.50 ± 1.59 trials to meet criterion, MAM/GFP = 18.33 ± 1.59 trials; Holm–Sidak saline/GFP vs MAM/GFP *t* = 2.16, *p* < 0.05). Inactivation of the vHipp-Nac pathway had no effect on extradimensional set-shifting in either the saline- or MAM-treated groups (saline/Gi = 13.17 ± 1.59 trials, MAM/Gi = 18.43 ± 1.47 trials; Holm–sidak saline/GFP vs saline/Gi *t* = 0.15, *p* > 0.05; Holm–Sidak MAM/GFP vs MAM/Gi *t* = 0.04, *p* > 0.05).

Conversely, hyperactivity in the vHipp-mPFC pathway is responsible for MAM-induced deficits in extradimensional set-shifting (Fig. 5d; two-way ANOVA: Interaction $F_{(1,23)} = 5.99$, *p* < 0.05; Prenatal treatment $F_{(1,23)} = 5.54$, *p* < 0.05; DREADD condition $F_{(1,23)} = 3.45$, *p* > 0.05; *n* = 6–7 per group). As expected, MAM-treated animals showed a deficit in extradimensional

set-shifting (saline/GFP = 11.286 ± 1.63 , MAM/GFP = 19.8 ± 1.93 ; Holm–Sidak saline/GFP vs MAM/GFP $t = 3.37$, $p < 0.05$). Although inhibition of the vHipp–mPFC pathway had no effect in saline-treated animals, it completely abolished the MAM-induced deficit in extradimensional set-shifting (saline/Gi = 12.33 ± 1.76 , MAM/Gi = 12.17 ± 1.76 ; Holm–Sidak saline/GFP vs saline/Gi $t = 0.44$, $p > 0.05$; Holm–Sidak MAM/GFP vs MAM/Gi $t = 2.92$, $p < 0.05$). Performance on all stages of the AST are shown in Fig. 5e, f. Together, these results suggest that hyperactivity in the vHipp–mPFC pathway, but not the vHipp–NAc pathway, contributes to the schizophrenia-like deficits in extradimensional set-shifting observed in MAM-treated animals.

Discussion

We, and others, have shown previously that hyperactivity in the ventral hippocampus (vHipp) is responsible for schizophrenia-like deficits in a variety of rodent models^{14,25}. Furthermore, normalizing hippocampal activity by transplanting GABAergic interneurons can attenuate behavioral deficits that model positive and cognitive symptoms of the disorder¹⁵. In the current study, we utilized a virally-mediated genetic approach to demonstrate that targeting tonic GABA signaling in pyramidal cells of the vHipp can normalize aberrant hippocampal activity and attenuate schizophrenia-like deficits. Specifically, we demonstrate that overexpression of the $\alpha 5$ subunit of the GABA_A receptor in pyramidal cells of the vHipp attenuates dopamine cell activity, which is related to positive symptoms of schizophrenia, and reverses behavioral deficits in cognitive flexibility. Further, we identified a potential mechanism by which vHipp pyramidal cell hyperactivity may affect distinct symptom domains associated with schizophrenia and other psychiatric diseases. Specifically, hyperactivity in projections from the vHipp to the NAc contribute to the aberrant increases in dopamine cell activity and is responsible for deficits in dopamine-dependent behaviors. Conversely, hyperactivity in projections to the mPFC have no effect on dopamine cell activity or related behaviors, but are responsible for some forms of cognitive inflexibility. Together, our results suggest that using gene therapy to restore GABAergic signaling in pyramidal cells of the vHipp may reduce activity in projections from the vHipp and may be a viable treatment strategy for targeting multiple symptom domains of schizophrenia.

Gene therapy, the method of using a viral vector to insert a gene directly into a cell, has shown great promise in recent years to not just treat symptoms but to actually cure certain diseases. For example, in Parkinson's Disease (PD), adeno-associated virus was used to over-express the GABA synthesizing enzyme, glutamic acid decarboxylase, in the subthalamic nucleus. The unilateral infusion reduced metabolism in the thalamus and ipsilateral motor and premotor cortices, which was correlated with improved clinical disability ratings. These effects were still apparent at 1 year and were not associated with severe side effects²⁶. In the current experiments, we used a lentiviral vector to over-express the $\alpha 5$ subunit of the GABA_A receptor. Lentivirus has also been used in PD patients to express tyrosine hydroxylase, GTP cyclohydrolase, and aromatic acid decarboxylase, three enzymes needed for dopamine synthesis, in striatal neurons. This treatment resulted in an improved motor score for up to 1 year²⁷. Further, in the current experiments, we demonstrate that we can improve multiple symptom domains by targeting a single brain region, the vHipp, reducing the possibility of negative side effects. However, further investigation of the long-term safety will be required before this treatment strategy can be moved to the clinic.

In the current experiments, we used viral-mediated gene transfer to increase expression of the $\alpha 5$ subunit of the GABA_A receptor. GABA_A receptors are heteropentameric chloride ion

channels with 19 known subunits ($\alpha 1$ – 6 , $\beta 1$ – 3 , $\gamma 1$ – 3 , δ , ϵ , π , θ , $\rho 1$ – 3). The $\alpha 5$ subunit is unique as its expression is primarily limited to the hippocampus¹⁶, making it an ideal target for specifically reducing the hippocampal hyperactivity associated with schizophrenia. Further, the $\alpha 5$ subunit has been identified primarily extrasynaptically in dendritic fields¹⁶, where it is thought to mediate tonic inhibitory currents²⁸. Indeed, in the current experiments, we demonstrate that over-expressing the $\alpha 5$ subunit increases tonic inhibitory currents in pyramidal cells of the vHipp. Further, we show that $\alpha 5$ overexpression also decreases the firing rate of hippocampal pyramidal cells, which is not surprising as tonic inhibition is thought to coordinate spike timing of pyramidal neurons and balance excitation¹⁷. By over-expressing the $\alpha 5$ subunit of the GABA_A receptor, we normalized pyramidal cell activity in the vHipp.

In addition, we demonstrated that $\alpha 5$ overexpression normalizes VTA dopamine cell population activity in the MAM model. Hyperactivity in the dopamine system is thought to underlie the positive symptoms of schizophrenia. For example, antipsychotic medications that block dopamine D2 receptors effectively reduce positive symptoms of the disorder²⁹. Further, elevated dopamine levels have been observed in the striatum of schizophrenia patients, and these levels have been correlated to the severity of positive symptoms³⁰. Drugs that increase dopamine signaling can induce psychotic episodes in schizophrenia patients³¹. The current results are in line with previous work demonstrating that administration of the $\alpha 5$ partial agonist, SH-053-2'F-R-CH₃, normalizes the number of spontaneously active dopamine neurons and amphetamine-induced locomotor activity in MAM rats²⁰. Further, others have shown that $\alpha 5$ knockout mice exhibit deficits in sensorimotor gating and latent inhibition^{18,19}. Together, this data suggest that increasing $\alpha 5$ expression in the vHipp may act through the dopamine system to alleviate positive symptoms of schizophrenia. It is important to note that in animal models of schizophrenia, positive symptoms seem to result from increases in dopamine signaling specifically in ventral regions of the striatum, including the NAc³². However, in human studies, imaging techniques, such as positron emission tomography, have demonstrated that the largest changes in dopamine signaling are actually observed in associative regions of the striatum³³. The reason for this discrepancy is a current area of research that remains to be elucidated.

In addition to dopamine cell activity, we also tested the ability of $\alpha 5$ subunit overexpression to improve schizophrenia-like deficits in cognitive function. We were surprised to find that $\alpha 5$ overexpression had no effect on reversal learning, one form of cognitive flexibility that is disrupted in schizophrenia. Reversal learning has been associated with dopamine signaling. For example, reversal learning performance is correlated with striatal dopamine synthesis capacity³⁴ and striatal D2 receptor availability³⁵. Dopamine depletion in the caudate nucleus impairs reversal learning³⁶. Further, both pharmacological agonism³⁷ and antagonism³⁸ of D2/D3 receptors can disrupt reversal learning, suggesting that this type of cognitive flexibility requires tightly controlled dopamine signaling. Because gene therapy normalized dopamine cell activity, we expected to see an improvement in reversal learning performance. Conversely, we did find that our gene therapy strategy attenuated the schizophrenia-like deficit in attentional set-shifting, a higher order form of cognitive flexibility mediated primarily by the medial prefrontal cortex (mPFC)²⁴. These results suggest that gene therapy to over-express the $\alpha 5$ subunit of the GABA_A receptor in pyramidal cells of the vHipp may be a viable treatment strategy to target some cognitive symptoms of schizophrenia, which have a profound impact on daily function^{1–3} but are poorly treated by currently available antipsychotic medications^{3,5}.

In the current experiments, we chose to focus on the hippocampus as both in schizophrenia patients and in animal models of schizophrenia, the hippocampus has been shown to be a key site of pathology. Decreases in hippocampal volume have been observed in schizophrenia patients at the time of first episode and seem to progress throughout the course of the illness³⁹. These decreases in volume are primarily limited to the anterior hippocampus⁴⁰, the sub-region of the hippocampus that corresponds to the ventral hippocampus of rodents^{41,42}. Further, unmedicated schizophrenia patients show increased hippocampal activity at rest⁷, an effect that is attenuated by antipsychotic treatment⁴³. Work in multiple animal models of schizophrenia has also demonstrated hyperactivity in the ventral hippocampus. For example, vHipp hyperactivity has been observed in developmental¹⁴, genetic⁴⁴, and pharmacological models²⁵ of schizophrenia. Further, we and others have shown that reducing hippocampal activity by transplanting inhibitory interneurons can normalize positive and cognitive symptoms of the disorder^{15,44}. In the current studies, we expanded on these findings to identify the neural circuits from the vHipp that influence specific aspects of schizophrenia-like behavior. The concept that unique symptom clusters can arise from disruptions in subcortical structures, which then lead to abnormal regulation of cortical activity and dopamine system function, has been previously proposed by O'Donnell and Grace⁴⁵. In order to test this hypothesis by manipulating discrete pathways from the vHipp we used chemogenetics, a method in which small molecule chemical actuators specifically interact with engineered proteins to affect the activity of a cell, such as G-protein-coupled receptors (GPCRs)⁴⁶. Specifically, we used the Designer Receptor Exclusively Activated by Designer Drugs (DREADD), hM4Di, a modified M4 muscarinic acetylcholine receptor that couples to the inhibitory Gi pathway when activated by clozapine-N-oxide, a highly selective, but pharmacologically inert, exogenous ligand⁴⁷. The hM4Di DREADD has been shown to silence neurons by hyperpolarizing the cell via activation of G-protein inwardly rectifying potassium channels (GIRKs)^{47,48} and inhibiting pre-synaptic neurotransmitter release⁴⁹. In the current experiments, we used an adeno-associated viral vector to over-express the inhibitory DREADD in cells of the vHipp, then injected CNO directly into the NAc or mPFC to specifically inhibit vHipp neurons that project to these regions. Although CNO is often administered systemically to inhibit activity in discrete brain regions, this pathway-targeting strategy has been used successfully by others⁵⁰.

One way in which the vHipp may influence schizophrenia-like behavior is through its control of the dopamine system⁴⁵. In rodents, the vHipp can regulate dopamine signaling via a polysynaptic pathway from the NAc to the ventral pallidum (VP), and ultimately to dopamine cells in the ventral tegmental area (VTA)⁵¹. Specifically, the vHipp regulates the dopamine neuron population activity, or the number of spontaneously active dopamine neurons, which has been correlated with dopamine efflux in the NAc³². Importantly, it has been shown that only spontaneously active dopamine neurons can respond to stimuli by firing in a bursting pattern⁵². In this way, the vHipp is thought to regulate the 'gain' of the dopamine system⁶. In the current studies, we demonstrate that hyperactivity in the vHipp-NAc pathway of MAM animals increases dopamine population activity in the VTA by showing a reduction in the number of spontaneously active dopamine cells per track after inhibition of the vHipp-NAc pathway.

Interestingly, we also found that inhibition of the vHipp-NAc pathway attenuates MAM-induced deficits in reversal learning. This is in contrast to the alpha 5 overexpression experiment, which also normalized dopamine cell activity in the VTA but did

not improve reversal learning in MAM-treated rats. Therefore, it is unlikely that inhibition of the vHipp-NAc pathway in MAM-treated animals improved reversal learning by normalizing dopamine activity in the striatum. However, other neurotransmitter systems and brain circuits have been implicated in reversal learning, including serotonin signaling in the orbital frontal cortex (OFC)²³. Furthermore, impacting the OFC-NAc pathway could occur either by normalization of vHipp-NAc activity or normalization of VTA-NAc activity. Further experiments are required to conclusively determine which specific pathways and neurotransmitters are associated with the effect of vHipp-NAc on reversal learning.

In addition to its projection to the NAc, the vHipp also projects directly to the prefrontal cortex⁵³, a brain region that has been implicated in the cognitive symptoms of schizophrenia⁵⁴. Schizophrenia patients show reduced prefrontal cortex activation during working memory tasks, with activation levels correlated to performance⁵⁵. Even schizophrenia patients that perform normally on working memory tasks show higher levels of PFC activation compared to controls, suggesting a deficit in efficiency⁵⁶. Further, anatomical changes, such as reduced dendritic spine density have been observed the PFC of schizophrenia patients⁵⁷. In line with these findings, we demonstrated that reducing hyperactivity in the vHipp-mPFC pathway improved attentional set-shifting performance in MAM-treated rats. This is not surprising as the mPFC has been implicated in this form of cognitive flexibility²⁴.

In the current experiments, we did not observe an effect of vHipp-mPFC pathway inhibition on dopamine population activity. However, it should be noted that we have previously demonstrated that synchronous cortical burst firing of the mPFC can increase dopamine population activity in the VTA⁵⁸. These studies also demonstrated that tonic activation of the mPFC produced subtle changes in VTA dopamine neurons suggesting that the effects of mPFC inhibition on VTA dopamine neuron activity would only be observed during periods of cortical burst firing.

In the current experiments, we focused on pathways from the vHipp to the NAc and mPFC. However, schizophrenia is a heterogeneous disorder and the vHipp is not the only site of pathology. For example, structural and functional changes have also been observed in the thalamus of schizophrenia patients⁵⁹ and we have recently demonstrated that the paraventricular nucleus of the thalamus can also regulate dopamine signaling via the NAc⁶⁰. Further, the vHipp sends and receives many projections to and from other brain regions beyond the NAc and mPFC. For example, reciprocal connections exist between the basolateral amygdala (BLA) and vHipp⁶¹ and optogenetic inhibition of this BLA-vHipp pathway has been shown to decrease anxiety-like behavior⁶² and increase social interaction time⁶³, which has been used to model negative symptoms of the disorder. Conversely, activation of the pathway increases anxiety-like behaviors⁶² and decreases social interaction time⁶³. The BLA has been implicated in schizophrenia⁶⁴, therefore, it is likely that changes in this neural circuit may also contribute to the pathology of schizophrenia. However, schizophrenia is a complex disorder and the individual pathways examined do not exist in isolation. Further, each patient experiences a unique set of symptoms. Therefore, we and other believe that symptom clusters in schizophrenia result from disruptions in interconnected neural systems involving the pathways examined in the current experiments⁴⁵.

In conclusion, we have demonstrated that normalizing hippocampal activity using a gene therapy strategy to over-express the $\alpha 5$ subunit of the GABA_A receptor in pyramidal cells can attenuate schizophrenia-like deficits in a rodent model. Further,

we showed that discrete projections from the vHipp differentially mediate symptoms of the disorder. We believe that by better understanding the neuronal pathways associated with discrete dimensions of antipsychotic efficacy, novel therapeutics can be developed with improved efficacy at treating multiple symptom domains associated with schizophrenia.

Methods

Animals. All experiments were performed in accordance with the guidelines outlined in the USPH Guide for the Care and Use of Laboratory Animals and were approved by the Institutional Animal Care and Use Committee of the University of Texas Health Science Center at San Antonio. Rats were maintained on a 12 h/12 h light/dark cycle, with food and water available *ad libitum* unless specified below.

MAM administration. To model circuit level alterations and behavioral deficits associated with schizophrenia, timed pregnant female Sprague–Dawley rats were obtained from Harlan on gestational day 16. Methylazoxymethanol (22 mg/kg i.p.) or saline was administered on gestational day 17, a dose and time point that induces schizophrenia-like changes in behavior and neuronal activity¹². Male pups were weaned on postnatal day 21 and housed in groups of 3 until they were >12 weeks old, at which point rats were singly housed and used for behavioral or electrophysiological experiments. All experiments included pups from multiple litters.

Stereotaxic surgeries. To over-express the $\alpha 1$ or $\alpha 5$ subunit of the GABA_A receptor under the control of the CAMKII promoter, lentiviral vectors were used. On postnatal days 40–45, animals were anesthetized using Fluriso (2–5% Isoflurane, USP with oxygen flow at 1 L/min) and placed in a stereotaxic apparatus. Bilateral cannula aimed at the vHipp (A/P + 4.8, M/L \pm 4.8, D/V –6.0 mm from bregma as determined using⁷⁰) were used to inject the $\alpha 1$ virus (pLV-CAMKII-rGabra1-IRES-EGFP; 3.19×10^9 TU/ml), $\alpha 5$ virus (pLV-CAMKII-rGabra5-IRES-EGFP; 2.86×10^9 TU/ml) or the control virus (pLV-EGFP:T2A-puro-EF1A > mcherry; 1.26×10^9 TU/ml) into each hemisphere (1.0 μ l; VectorBuilder). Animals were allowed to recover for >6 weeks before behavioral and electrophysiological experiments to allow maximal gene expression.

To over-express the designer receptor hm4D (Gi), a modified version of the human Gi-coupled muscarinic receptor 4 that inhibits neuronal activity in response to the exogenous ligand, clozapine-N-oxide⁴⁷, AAV2 vectors driven by the CAMKII promoter were used. On postnatal days 40–45, animals were anesthetized (Fluriso), placed in a stereotaxic apparatus and bilateral cannula were used to inject the Gi virus (RAAV2-CAMKII α -HA-hM4D(Gi)-IRES-mcitrine; 1.4×10^{12} vm/ml, 1.0 μ l) or the control virus (RAAV2-CAMKII α -eYFP; 3.8×10^{12} vm/ml; 1 μ l; UNC Vector Core) into each vHipp (A/P + 4.8, M/L \pm 4.8, D/V –6.0 mm from bregma).

Five weeks after the virus injections, bilateral guide cannula were implanted directly above the NAc (A/P + 1.4, M/L \pm 1.3, DV –6.6 mm from bregma as determined using⁷⁰) or the mPFC (A/P + 3.0, M/L \pm 0.6, DV –3.5 mm from bregma as determined using⁷⁰), and secured to the skull using dental cement and four anchor screws. Animals were allowed at least one week to recover before behavioral or electrophysiological experiments were performed. The pathway inhibition strategy is depicted in Fig. 4a, b.

Whole-cell patch-clamp recordings. It is well known that ectopic expression of receptors may not necessarily recapitulate the physiological role of that receptor *in vivo*. To better understand the consequence of $\alpha 1$ and $\alpha 5$ overexpression in vHipp pyramidal neurons, we employed whole-cell patch-clamp electrophysiology. Brains were removed and placed in ice-cold artificial cerebrospinal fluid (aCSF) containing (in mM): 261 sucrose, 2 KCl, 2 MgSO₄, 1.25 NaH₂PO₄, 1 CaCl₂, 1 MgCl₂, 10 HEPES, 10 glucose, and 0.4 ascorbic acid (pH 7.4, 315 mOsm). Brains were cut into horizontal 300 μ m slices with a Vibratome (Leica Microsystems, Wetzlar, Germany). Slices contain the hippocampus were incubated in standard aCSF containing (in mM): 140 NaCl, 2.5 KCl, 2 CaCl₂, 1 MgCl₂, 10 HEPES, 10 glucose, and 0.4 ascorbic acid (pH 7.4, 295 mOsm) at room temperature for at least 1 h before recording commenced.

Patch-clamp recordings from hippocampal CA1 pyramidal neurons were performed with the aid of IR-DIC optics and a 16-bit EMCCD digital camera (Photometrics, Inc.). Patch electrodes were pulled (Flaming/Brown P-97, Sutter Instrument, Novato, CA, USA) from borosilicate glass capillaries and polished to a tip resistance of 3–5 M Ω . Electrodes were filled with a solution containing (in mM): 120 CsCl, 1 MgCl₂, 10 HEPES, 1 EGTA, 4 NaCl, 2 Mg-ATP, 5 QX-314 (pH 7.2, 287 mOsm). Tonic GABA currents and spontaneous IPSC activity were recorded in whole-cell configuration in voltage-clamp mode ($V_{\text{hold}} = -70$ mV) using an Axopatch 200B amplifier and pCLAMP software (v10.3, Axon Instruments, Union City, CA, USA). Signals were filtered at 2 kHz, digitized 10 kHz (Digidata 1440 A, Axon Instruments), and saved on a computer for offline analysis. Recordings were made from neurons identified by the AAV-encoded fluorescent reporter GFP using an appropriate filter set. Recordings were performed with AMPA and NMDA receptors blocked with CNQX (10 μ M) and DL-AP5 (50 μ M),

respectively. Tonic GABA current was measured as a reduction of holding current following bath application of picrotoxin (100 μ M) for ~5 min. Amplitude and frequency of sIPSC activity were quantified using Clampfit software (v10.3) from ~3 min of stable baseline data recorded at least 5 min after achieving whole-cell configuration and prior to picrotoxin exposure.

Extracellular dopamine recordings. To measure the activity of dopamine neurons in the ventral tegmental area (VTA), rats were anesthetized with 8% chloral hydrate (400 mg kg⁻¹, i.p.), which does not appreciably affect dopamine system function⁶⁵. Rats were then placed in a stereotaxic apparatus. Supplemental anesthesia was administered as necessary and a core body temperature of 37 °C was maintained. Extracellular glass microelectrodes were lowered into the VTA (A/P –5.3, M/L \pm 0.6, D/V –6.5 to 9.0 from bregma as determined using⁷⁰) using a hydraulic microdrive. Previously established electrophysiological criteria were used to identify spontaneously active dopamine neurons⁶⁶ encountered while making 6–9 vertical passes through the VTA. Neuronal activity was filtered (high-frequency cutoff: 30 kHz, low-frequency cutoff: 30 Hz) and recorded using LabChart software (version 7.1; ADInstruments, Chalgrove, Oxfordshire, UK). It should be noted that; while dopamine neurons projecting to different brain regions display distinct electrophysiological signatures⁶⁷, the ability to physiologically identify dopamine neurons *in vivo* has been recently confirmed in a review by Ungless and Grace⁶⁸. The following parameters of dopamine neuron activity were analyzed: (1) population activity, which was defined as the average number of spontaneously active neurons recorded per electrode track, (2) basal firing rate, and (3) the proportion of action potentials occurring in bursts (bursts defined as the occurrence of two spikes with an interspike interval of 80 ms, and the termination of the burst defined as the occurrence of an interspike interval of 160 ms).

Extracellular pyramidal cell recordings. In order to measure putative pyramidal cell activity in the vHipp, we performed *in vivo* extracellular recordings as described above. Extracellular glass microelectrodes were lowered into the vHipp (A/P –5.0, M/L \pm 4.5, D/V –4.0–8.0 from bregma) and putative pyramidal neurons (identified by a firing rate <2 Hz⁶⁹) were recorded. The firing rate was analyzed using Labchart software.

CNO injections. On the day of behavioral testing, animals were moved to the behavioral facility and allowed at least 1 h to acclimatize. Approximately 15 min prior to testing, bilateral microinjectors (Plastics One) that extended 1 mm past the end of the indwelling cannula were used to inject 300 μ M (0.75 μ l, dissolved in saline) CNO into the NAc or mPFC.

Attentional set-shifting test. To measure cognitive flexibility, the AST was used. Rats were restricted to 12 g food/day for 7 days prior to testing. Using a cheerio reward, rats were trained to dig in pots defined by cues along two stimulus dimensions: the digging medium filling the pot and an odor (Aura Cacia essential oils) applied to the inner rim of the pot. During testing, the rat was taken through a series of stages, each requiring a different discrimination, with a criterion of six consecutive correct trials required to proceed to the next stage. The first stage was a simple discrimination (SD), with only one stimulus dimension (odor or medium) present. Odor (clove or nutmeg) was the initial relevant dimension (signaling the location of the reward) for half the animals, and medium (raffia or yarn) for the other half. The second stage was a compound discrimination (CD) in which the same discrimination was required and the second irrelevant dimension was introduced. The third stage was a reversal (R1) in which the same odors and media were used, and the same dimension remained relevant, but the negative cue from the previous stage became positive and the positive cue from the previous stage was now negative. Stage 4 was an intradimensional shift (ID), in which all new odors (cinnamon or rosemary) and media (beads or wood balls) were introduced but the same dimension remained relevant. After performing a second reversal (R2), the last stage was an extradimensional set-shift (ED). During ED, all new odors (citronella or thyme) and media (velvet or crepe paper) were presented and the previously irrelevant stimulus became relevant.

Immunohistochemistry. Immunohistochemistry was used to confirm virus-mediated gene expression in vHipp neurons. Briefly, after behavioral and physiological experiments were performed, rats were transcardially perfused with saline, followed by 4% paraformaldehyde. Brains were post-fixed and cryoprotected in 10% sucrose in phosphate-buffered saline (PBS). For antigen retrieval, free-floating coronal sections from the vHipp (50 μ m) were boiled in 10 mM citric acid, pH 6, for a total of 5 min. Sections were then washed in PBS, blocked (2% normal goat serum and 0.3% Triton X-100), then incubated with chicken anti-GFP antibody (Millipore; 1:1000) at 4 °C overnight. Sections were then incubated with AlexaFluor 488 goat anti-chicken secondary antibody (1:1000). To confirm pyramidal cell expression, a subset of sections were then incubated with mouse anti-CAMKII antibody (Thermo Fisher; 1:200) followed by AlexaFluor 594 goat anti-mouse (1:1000). Sections were mounted on slides and cover-slipped using Prolong gold anti-fade reagent. Sections were imaged using an Olympus IX81 Motorized Inverted microscope. The representative images were acquired using FV10-ASW software and enhanced using ImageJ.

Statistics. Animals were randomly assigned to treatment groups. In all figures, data are shown as mean \pm SEM and n is indicated in the figure legend. In the patch-clamp experiments, data were analyzed using a one-way ANOVA followed by the Holm–Sidak post-hoc test. For all other experiments, data were analyzed using a two-way ANOVA and Holm–Sidak post-hoc test. All tests were two tailed and significance was determined to at $p < 0.05$.

Reporting summary. Further information on research design is available in the Nature Research Reporting Summary linked to this article.

Data availability

The datasets generated during and/or analyzed during the current study are available from the corresponding author upon reasonable request.

Received: 4 October 2018 Accepted: 29 May 2019

Published online: 27 June 2019

References

- Strassnig, M. T. et al. Determinants of different aspects of everyday outcome in schizophrenia: the roles of negative symptoms, cognition, and functional capacity. *Schizophr. Res.* <https://doi.org/10.1016/j.schres.2015.03.033> (2015).
- Green, M. F., Kern, R. S., Braff, D. L. & Mintz, J. Neurocognitive deficits and functional outcome in schizophrenia. *Schizophr. Bull.* **26**, 119–136 (2000).
- Citrome, L. Unmet needs in the treatment of schizophrenia: new targets to help different symptom domains. *J. Clin. psychiatry* **75**, 21–26 (2014). Suppl. 1.
- Carpenter, W. T. Jr. & Davis, J. M. Another view of the history of antipsychotic drug discovery and development. *Mol. Psychiatry* **17**, 1168–1173 (2012).
- Leucht, S. et al. Comparative efficacy and tolerability of 15 antipsychotic drugs in schizophrenia: a multiple-treatments meta-analysis. *Lancet* **382**, 951–962 (2013).
- Lodge, D. J. & Grace, A. A. Hippocampal dysregulation of dopamine system function and the pathophysiology of schizophrenia. *Trends Pharmacol. Sci.* **32**, 507–513 (2011).
- Medoff, D. R., Holcomb, H. H., Lahti, A. C. & Tamminga, C. A. Probing the human hippocampus using rCBF: contrasts in schizophrenia. *Hippocampus* **11**, 543–550 (2001).
- Schobel, S. A. et al. Differential targeting of the ca1 subfield of the hippocampal formation by schizophrenia and related psychotic disorders. *Arch. Gen. Psychiatry* **66**, 938–946 (2009).
- Heckers, S. & Konradi, C. GABAergic mechanisms of hippocampal hyperactivity in schizophrenia. *Schizophr. Res.* <https://doi.org/10.1016/j.schres.2014.09.041> (2014).
- Zhang, Z. J. & Reynolds, G. P. A selective decrease in the relative density of parvalbumin-immunoreactive neurons in the hippocampus in schizophrenia. *Schizophr. Res.* **55**, 1–10 (2002).
- Konradi, C. et al. Hippocampal interneurons are abnormal in schizophrenia. *Schizophr. Res.* **131**, 165–173 (2011).
- Lodge, D. J. The MAM Rodent Model of Schizophrenia. *Current protocols in neuroscience*. **63**, 9.43.41–49.43.47, <https://doi.org/10.1002/0471142301.ns0943s63> (2013).
- Lodge, D. J., Behrens, M. M. & Grace, A. A. A loss of parvalbumin-containing interneurons is associated with diminished oscillatory activity in an animal model of schizophrenia. *J. Neurosci.* **29**, 2344–2354 (2009).
- Lodge, D. J. & Grace, A. A. Aberrant hippocampal activity underlies the dopamine dysregulation in an animal model of schizophrenia. *J. Neurosci.* **27**, 11424–11430 (2007).
- Donegan, J. J. et al. Stem cell derived interneuron transplants as a treatment for schizophrenia: preclinical validation in a rodent model. *Mol. Psychiatry*. <https://doi.org/10.1038/mp.2016.121> (2016).
- Fritschy, J.-M. & Mohler, H. GABAA-receptor heterogeneity in the adult rat brain: differential regional and cellular distribution of seven major subunits. *J. Comp. Neurol.* **359**, 154–194 (1995).
- Semyanov, A., Walker, M. C., Kullmann, D. M. & Silver, R. A. Tonic active GABAA receptors: modulating gain and maintaining the tone. *Trends Neurosci.* **27**, 262–269 (2004).
- Gerdjikov, T. V. et al. Hippocampal $\alpha 5$ subunit-containing GABAA receptors are involved in the development of the latent inhibition effect. *Neurobiol. Learn. Mem.* **89**, 87–94 (2008).
- Hauser, J. et al. Hippocampal $\alpha 5$ subunit-containing GABAA receptors modulate the expression of prepulse inhibition. *Mol. Psychiatry* **10**, 201 (2004).
- Gill, K. M., Lodge, D. J., Cook, J. M., Aras, S. & Grace, A. A. A novel [alpha] 5GABAAR-positive allosteric modulator reverses hyperactivation of the dopamine system in the MAM model of schizophrenia. *Neuropsychopharmacology* **36**, 1903–1911 (2011).
- Blits, B. & Petry, H. Perspective on the road toward gene therapy for Parkinson’s disease. *Front. Neuroanat.* **10**, 128 (2016).
- Serwanski, D. R. et al. Synaptic and nonsynaptic localization of GABAA receptors containing the $\alpha 5$ subunit in the rat brain. *J. Comp. Neurol.* **499**, 458–470 (2006).
- Kehagia, A. A., Murray, G. K. & Robbins, T. W. Learning and cognitive flexibility: frontostriatal function and monoaminergic modulation. *Curr. Opin. Neurobiol.* **20**, 199–204 (2010).
- Birrell, J. M. & Brown, V. J. Medial frontal cortex mediates perceptual attentional set shifting in the rat. *J. Neurosci.* **20**, 4320–4324 (2000).
- Aguilar, D. D., Chen, L. & Lodge, D. J. Increasing endocannabinoid levels in the ventral pallidum restore aberrant dopamine neuron activity in the subchronic PCP rodent model of schizophrenia. *Int. J. Neuropsychopharmacol.* <https://doi.org/10.1093/ijnp/pyu035> (2015).
- Feigin, A. et al. Modulation of metabolic brain networks after subthalamic gene therapy for Parkinson’s disease. *Proc. Natl Acad. Sci. USA* **104**, 19559–19564 (2007).
- Palfi, S. et al. Long-term safety and tolerability of ProSavin, a lentiviral vector-based gene therapy for Parkinson’s disease: a dose escalation, open-label, phase 1/2 trial. *Lancet* **383**, 1138–1146 (2014).
- Bai, D. et al. Distinct functional and pharmacological properties of tonic and quantal inhibitory postsynaptic currents mediated by gamma-aminobutyric acid(A) receptors in hippocampal neurons. *Mol. Pharmacol.* **59**, 814–824 (2001).
- Seeman, P., Chau-Wong, M., Tedesco, J. & Wong, K. Brain receptors for antipsychotic drugs and dopamine: direct binding assays. *Proc. Natl Acad. Sci. USA* **72**, 4376–4380 (1975).
- Abi-Dargham, A. et al. Increased baseline occupancy of D2 receptors by dopamine in schizophrenia. *Proc. Natl Acad. Sci. USA* **97**, 8104–8109 (2000).
- Janowsky, D. S., El-Yousef, M., Davis, J. M. & Sekerke, H. Provocation of schizophrenic symptoms by intravenous administration of methylphenidate. *Arch. Gen. Psychiatry* **28**, 185–191 (1973).
- Floresco, S. B., West, A. R., Ash, B., Moore, H. & Grace, A. A. Afferent modulation of dopamine neuron firing differentially regulates tonic and phasic dopamine transmission. *Nat. Neurosci.* **6**, 968–973 (2003).
- McCutcheon, R., Beck, K., Jauhar, S. & Howes, O. D. Defining the locus of dopaminergic dysfunction in schizophrenia: a meta-analysis and test of the mesolimbic hypothesis. *Schizophr. Bull.* **44**, 1301–1311 (2017).
- Cools, R. et al. Striatal dopamine predicts outcome-specific reversal learning and its sensitivity to dopaminergic drug administration. *J. Neurosci.* **29**, 1538–1543 (2009).
- Jocham, G. et al. Dopamine DRD2 polymorphism alters reversal learning and associated neural activity. *J. Neurosci.* **29**, 3695–3704 (2009).
- Clarke, H. F., Hill, G. J., Robbins, T. W. & Roberts, A. C. Dopamine, but not serotonin, regulates reversal learning in the marmoset caudate nucleus. *J. Neurosci.* **31**, 4290–4297 (2011).
- Boulougouris, V., Castañé, A. & Robbins, T. Dopamine D2/D3 receptor agonist quinpirole impairs spatial reversal learning in rats: investigation of D3 receptor involvement in persistent behavior. *Psychopharmacology* **202**, 611–620 (2009).
- Lee, B., Groman, S., London, E. D. & Jentsch, J. D. Dopamine D2/D3 receptors play a specific role in the reversal of a learned visual discrimination in monkeys. *Neuropsychopharmacology* **32**, 2125–2134 (2007).
- Velakoulis, D. et al. Hippocampal and amygdala volumes according to psychosis stage and diagnosis: a magnetic resonance imaging study of chronic schizophrenia, first-episode psychosis, and ultra-high-risk individuals. *Arch. Gen. Psychiatry* **63**, 139–149 (2006).
- Szeszko, P. R. et al. Smaller anterior hippocampal formation volume in antipsychotic-naive patients with first-episode schizophrenia. *Am. J. Psychiatry* **160**, 2190–2197 (2003).
- Fanselow, M. S. & Dong, H.-W. Are the dorsal and ventral hippocampus functionally distinct structures? *Neuron* **65**, 7–19 (2010).
- Grace, A. A. Dopamine system dysregulation by the hippocampus: implications for the pathophysiology and treatment of schizophrenia. *Neuropharmacology* **62**, 1342–1348 (2012).
- Medoff, D. R., Holcomb, H. H., Lahti, A. C. & Tamminga, C. A. Probing the human hippocampus using rCBF: contrasts in schizophrenia. *Hippocampus* **11**, 543–550 (2001).
- Gilani, A. I. et al. Interneuron precursor transplants in adult hippocampus reverse psychosis-relevant features in a mouse model of hippocampal disinhibition. *Proc. Natl Acad. Sci. USA* **111**, 7450–7455 (2014).

45. O'Donnell, P. & Grace, A. A. Dysfunctions in multiple interrelated systems as the neurobiological bases of schizophrenic symptom clusters. *Schizophr. Bull.* **24**, 267–283 (1998).
46. Roth, B. L. DREADDs for neuroscientists. *Neuron* **89**, 683–694 (2016).
47. Armbruster, B. N., Li, X., Pausch, M. H., Herlitze, S. & Roth, B. L. Evolving the lock to fit the key to create a family of G protein-coupled receptors potentially activated by an inert ligand. *Proc. Natl Acad. Sci. USA* **104**, 5163–5168 (2007).
48. Vardy, E. et al. A new DREADD facilitates the multiplexed chemogenetic interrogation of behavior. *Neuron* **86**, 936–946 (2015).
49. Stachniak, T. J., Ghosh, A. & Sternson, S. M. Chemogenetic synaptic silencing of neural circuits localizes a hypothalamus→midbrain pathway for feeding behavior. *Neuron* **82**, 797–808 (2014).
50. Stachniak, T. J., Ghosh, A. & Sternson, S. M. Chemogenetic synaptic silencing of neural circuits localizes a hypothalamus→midbrain pathway for feeding behavior. *Neuron* **82**, 797–808 (2014).
51. Floresco, S. B., Todd, C. L. & Grace, A. A. Glutamatergic afferents from the hippocampus to the nucleus accumbens regulate activity of ventral tegmental area dopamine neurons. *J. Neurosci.* **21**, 4915–4922 (2001).
52. Lodge, D. J. & Grace, A. A. The hippocampus modulates dopamine neuron responsiveness by regulating the intensity of phasic neuron activation. *Neuropsychopharmacology* **31**, 1356–1361 (2006).
53. Jay, T. M. & Witter, M. P. Distribution of hippocampal CA1 and subicular efferents in the prefrontal cortex of the rat studied by means of anterograde transport of Phaseolus vulgaris-leucoagglutinin. *J. Comp. Neurol.* **313**, 574–586 (1991).
54. Bunney, W. E. & Bunney, B. G. Evidence for a compromised dorsolateral prefrontal cortical parallel circuit in schizophrenia. *Brain Res. Rev.* **31**, 138–146 (2000).
55. Weinberger, D. R., Berman, K. & Zec, R. F. Physiologic dysfunction of dorsolateral prefrontal cortex in schizophrenia: I. regional cerebral blood flow evidence. *Arch. Gen. Psychiatry* **43**, 114–124 (1986).
56. Callicott, J. H. et al. Complexity of prefrontal cortical dysfunction in schizophrenia: more than up or down. *Am. J. Psychiatry* **160**, 2209–2215 (2003).
57. Garey, L. J. et al. Reduced dendritic spine density on cerebral cortical pyramidal neurons in schizophrenia. *J. Neurol. Neurosurg. psychiatry* **65**, 446–453 (1998).
58. Lodge, D. J. The medial prefrontal and orbitofrontal cortices differentially regulate dopamine system function. *Neuropsychopharmacology* **36**, 1227–1236 (2011).
59. Pergola, G., Selvaggi, P., Trizio, S., Bertolino, A. & Blasi, G. The role of the thalamus in schizophrenia from a neuroimaging perspective. *Neurosci. Biobehav. Rev.* **54**, 57–75 (2015).
60. Perez, S. M. & Lodge, D. J. Convergent inputs from the hippocampus and thalamus to the nucleus accumbens regulate dopamine neuron activity. *J. Neurosci.* **38**, 10607–10618 (2018).
61. O'Donnell, P. & Grace, A. A. Synaptic interactions among excitatory afferents to nucleus accumbens neurons: hippocampal gating of prefrontal cortical input. *J. Neurosci.* **15**, 3622–3639 (1995).
62. Felix-Ortiz, A. C. et al. BLA to vHPC inputs modulate anxiety-related behaviors. *Neuron* **79**, 658–664 (2013).
63. Felix-Ortiz, A. C. & Tye, K. M. Amygdala inputs to the ventral hippocampus bidirectionally modulate social behavior. *J. Neurosci.* **34**, 586–595 (2014).
64. Shayegan, D. K. & Stahl, S. M. Emotion processing, the amygdala, and outcome in schizophrenia. *Prog. Neuropsychopharmacol. Biol. Psychiatry* **29**, 840–845 (2005).
65. Pan, W. H. & Lai, Y. J. Anesthetics decreased the microdialysis extraction fraction of norepinephrine but not dopamine in the medial prefrontal cortex. *Synapse* **21**, 85–92 (1995).
66. Grace, A. A. & Bunney, B. S. Intracellular and extracellular electrophysiology of nigral dopaminergic neurons—I. *Identif. Charact. Neurosci.* **10**, 301–315 (1983).
67. Lammel, S. et al. Unique properties of mesoprefrontal neurons within a dual mesocorticolimbic dopamine system. *Neuron* **57**, 760–773 (2008).
68. Ungless, M. A. & Grace, A. A. Are you or aren't you? Challenges associated with physiologically identifying dopamine neurons. *Trends Neurosci.* **35**, 422–430 (2012).
69. Ranck, J. B. J. Studies on single neurons in dorsal hippocampal formation and septum in unrestrained rats. I. Behavioral correlates and firing repertoires. *Exp. Neurol.* **41**, 461–531 (1973).
70. Paxinos, G. & Watson, C. *The Rat Brain in Stereotaxic Coordinates*. 6th edn, (Elsevier, 2007).

Acknowledgements

This work was supported by the Owens Foundation, R01 MH090067 (D.L.) from the National Institute for Mental Health, P01 HL088052 (G.T.) from the National Heart, Lung and Blood Institute, and by TL1TR002647 (J.D.) from the National Center for Advancing Translational Science. Images were generated in the Core Optical Imaging Facility which is supported by UTHSCSA, NIH-NCI P30 CA54174 (CTRC at UTHSCSA) and NIH-NIA P01AG19316. This content is solely the responsibility of the authors and does not necessarily represent the official views of the National Institutes of Health. We would like to thank Luke Thomas for his technical assistance.

Author contributions

J.D., D.L. and G.T. participated in research design. J.D., A.B. and J.Y. conducted experiments. J.D., D.L., J.Y. and G.T. performed the data analysis. All authors wrote or contributed to the writing of the manuscript.

Additional information

Supplementary Information accompanies this paper at <https://doi.org/10.1038/s41467-019-10800-1>.

Competing interests: The authors declare no competing interests.

Reprints and permission information is available online at <http://npg.nature.com/reprintsandpermissions/>

Peer review information: *Nature Communications* thanks Jasper Heinsbroek and the other, anonymous, reviewer(s) for their contribution to the peer review of this work. Peer reviewer reports are available.

Publisher's note: Springer Nature remains neutral with regard to jurisdictional claims in published maps and institutional affiliations.



Open Access This article is licensed under a Creative Commons Attribution 4.0 International License, which permits use, sharing, adaptation, distribution and reproduction in any medium or format, as long as you give appropriate credit to the original author(s) and the source, provide a link to the Creative Commons license, and indicate if changes were made. The images or other third party material in this article are included in the article's Creative Commons license, unless indicated otherwise in a credit line to the material. If material is not included in the article's Creative Commons license and your intended use is not permitted by statutory regulation or exceeds the permitted use, you will need to obtain permission directly from the copyright holder. To view a copy of this license, visit <http://creativecommons.org/licenses/by/4.0/>.

© The Author(s) 2019